

AtREC8 and AtSCC3 are essential to the monopolar orientation of the kinetochores during meiosis

Liudmila Chelysheva, Stéphanie Diallo*, Daniel Vezon, Ghislaine Gendrot, Nathalie Vrielynck, Katia Belcram, Nathalie Rocques, Angustias Márquez-Lema[‡], Anuj M. Bhatt[§], Christine Horlow, Raphaël Mercier, Christine Mézard and Mathilde Grelon[¶]

Institut Jean-Pierre Bourgin, Station de Génétique et d'Amélioration des Plantes, INRA de Versailles, Route de Saint-Cyr, 78026 Versailles CEDEX, France

*Present address: Laboratoire de Microbiologie du Froid UPRES 2123, 55 Rue Saint-Germain, 27000 Evreux, France

‡Present address: Instituto de Agricultura Sostenible (CSIC), Apartado 4084, E-14080, Córdoba, Spain

§Present address: Department of Plant Sciences, University of Oxford, South Parks Road, Oxford, OX1 3RB, UK

¶Author for correspondence (e-mail: grelon@versailles.inra.fr)

Accepted 13 July 2005

Journal of Cell Science 118, 4621–4632 Published by The Company of Biologists 2005

doi:10.1242/jcs.02583

Summary

The success of the first meiotic division relies (among other factors) on the formation of bivalents between homologous chromosomes, the monopolar orientation of the sister kinetochores at metaphase I and the maintenance of centromeric cohesion until the onset of anaphase II. The meiotic cohesin subunit, Rec8 has been reported to be one of the key players in these processes, but its precise role in kinetochore orientation is still under debate. By contrast, much less is known about the other non-SMC cohesin subunit, Scc3. We report the identification and the characterisation of *AtSCC3*, the sole *Arabidopsis* homologue of *Scc3*. The detection of *AtSCC3* in mitotic cells, the embryo lethality of a null allele *Atscc3-2*, and the mitotic defects of the weak allele *Atscc3-1* suggest that *AtSCC3* is required for mitosis. *AtSCC3* was also detected

in meiotic nuclei as early as interphase, and bound to the chromosome axis from early leptotene through to anaphase I. We show here that both *AtREC8* and *AtSCC3* are necessary not only to maintain centromere cohesion at anaphase I, but also for the monopolar orientation of the kinetochores during the first meiotic division. We also found that *AtREC8* is involved in chromosome axis formation in an *AtSPO11-1*-independent manner. Finally, we provide evidence for a role of *AtSPO11-1* in the stability of the cohesin complex.

Supplementary material available online at
<http://jcs.biologists.org/cgi/content/full/118/20/4621/DC1>

Key words: Cohesion, Scc3, Rec8, Spo11, *Arabidopsis*

Introduction

Accurate chromosome segregation during mitosis and meiosis is based on processes that are particularly well conserved among eukaryotes. One of these processes, sister chromatid cohesion, holds newly replicated chromatids together until anaphase. Mitotic cohesion is laid down during S phase and released at the metaphase-anaphase transition to allow chromatid segregation. Meiosis is a modified cell division in which a single S phase takes place before two rounds of chromosomal segregation. The homologous chromosomes are pulled to opposite poles of the cell at the first meiotic division (meiosis I), whereas the sister chromatids segregate only at meiosis II. A successful first meiotic division requires the association of homologous chromosomes as bivalents during prophase I, the monopolar attachment of sister kinetochores at metaphase I, and the preservation of centromere cohesion at anaphase I, when arm cohesion is released (reviewed by Watanabe, 2004).

Yeast mitotic cohesion depends on a multisubunit protein complex (the cohesin complex), comprising four essential proteins: Scc1, Scc3 and two members of the ubiquitous structural maintenance of chromosome (Smc) family: Smc1 and Smc3 (reviewed by Nasmyth, 2002). The cohesin complex

may be organised in a ring in which the Smc1/3 heterodimer forms a large V closed by Scc1 (Anderson et al., 2002; Gruber et al., 2003; Haering et al., 2002), probably with the aid of Scc3, which is thought to bind Scc1 (Nasmyth, 2002). At anaphase, Scc1 cleavage by an endopeptidase (separase) releases cohesion, allowing chromatids to segregate (Haering and Nasmyth, 2003). During meiosis, cohesion is released in two steps. First, at anaphase I, arm cohesion is released but centromere cohesion retained, facilitating the release of chiasmata and the segregation of homologues. Centromere cohesion is then released at anaphase II, allowing the sister chromatids to separate. The mechanisms controlling these processes are only now becoming clear. In all organisms studied, Scc1 is mostly replaced at meiosis by a meiotic orthologue (Rec8). And as far as we know, this replacement is absolutely necessary for the maintenance of centromeric cohesion at meiosis I (Klein et al., 1999; Watanabe and Nurse, 1999). The protection of centromeric Rec8 at anaphase I appears to be mediated by the Sgo1 protein, recently identified in yeasts (Katis et al., 2004; Kitajima et al., 2004), and widely conserved across different species (Watanabe, 2004). Unlike the clear role Rec8 plays in centromeric cohesion at meiosis I, the role of Rec8 in kinetochore orientation at meiosis I remains

ambiguous. Although it has been shown in *Schizosaccharomyces pombe* that Rec8 is required for kinetochores to be oriented to the same pole (Watanabe and Nurse, 1999; Watanabe et al., 2001; Yokobayashi et al., 2003), replacement of Rec8 by Scc1 in *Saccharomyces cerevisiae* preserves the monopolar orientation, showing that at least in this organism Rec8 is not obligatory for monopolar attachment of kinetochores (Toth et al., 2000). In other organisms, it has been difficult to assess whether Rec8 was involved or not in kinetochore orientations. So far, in all other organisms studied, Rec8 depletion either leads to an early release of cohesion (before metaphase I) or induces strong chromosome fragmentation (Bai et al., 1999; Bannister et al., 2004; Bhatt et al., 1999; Klein et al., 1999; Pasierbek et al., 2001).

Very few data are currently available for the other cohesin subunits, including Scc3. This protein was first identified as a member of the yeast mitotic cohesin complex (Toth et al., 1999) and was subsequently identified in *Caenorhabditis elegans*, the only organism in which this protein has been shown to play a role in both mitotic and meiotic cohesion (Pasierbek et al., 2003; Wang et al., 2003). In contrast to the sole Scc3 found in *S. cerevisiae* and in *C. elegans*, other organisms (*Drosophila melanogaster*, *S. pombe*, mammals, *Xenopus laevis*) possess several Scc3-like proteins. *S. pombe* has two Scc3-like proteins that play specific roles: Rec11 is involved in arm cohesion, whereas Psc3 is required for centromere cohesion during meiosis (Kitajima et al., 2003); only Psc3 has been shown to also be involved in mitotic cohesion (Tomonaga et al., 2000). The mammalian *STAG3* gene, which encodes one of three Scc3 homologues, has been shown to be specific to meiosis (Pezzi et al., 2000), where it is probably involved in meiosis I sister arm cohesion (Prieto et al., 2001) and may therefore be the homologue of Rec11.

In this study, we investigated the function of the sole *Arabidopsis* Scc3 homologue (*AtSCC3*) and demonstrated its involvement in both meiotic and mitotic divisions. Our results suggest that both cohesins, AtREC8 and AtSCC3, are necessary for the monopolar orientation of the kinetochores at meiosis I and for the maintenance of centromeric cohesion at anaphase I. Further, our study highlights possible differences between AtREC8 and AtSCC3 during recombination repair and axis building. Finally, we demonstrate a role for AtSPO11-1 in stabilisation of the cohesin complex.

Materials and Methods

Plant material

The *Atscc3-1* mutant (EDT1 line) was obtained from the Versailles collection of *Arabidopsis* T-DNA transformants (Ws accession) (Bechtold et al., 1993). Its FST was obtained from <https://genoplante.infobiogen.fr/flagdb/info>. The *Atscc3-2* mutant, line SALK_021769, was obtained from the collection of T-DNA mutants of the Salk Institute Genomic Analysis Laboratory (Col-0 accession) (SIGnAL, <http://signal.salk.edu/cgi-bin/tdnaexpress>) (Alonso et al., 2003) and provided by NASC (<http://nasc.nott.ac.uk/>). The *Atrec8* is *dif1-1* allele (Ler accession) is described elsewhere (Bhatt et al., 1999). The *Atspo11-1-1* mutant (Ws accession) is also described (Grelon et al., 2001).

Growth conditions

Arabidopsis plants were cultivated in a greenhouse or growth chamber

under a 16-hour day/8-hour night photoperiod, at 20°C with 70% humidity. For culture in vitro, sterilised seeds were plated on *Arabidopsis* medium (Estelle and Somerville, 1987) diluted 1:2. Plates were incubated for 48 hours at 4°C in the dark and were then transferred to the growth chamber. For primary root measurement, plates were stood on end.

Sequence analyses

Protein sequence similarity searches were performed at the National Center for Biotechnology Information (<http://www.ncbi.nlm.nih.gov/BLAST/>) and at the *Arabidopsis* Information Resource (TAIR, <http://www.arabidopsis.org/Blast>), using BLOSUM45 matrix and default parameters. Sequence analyses were performed with DNAssist software (<http://www.dnassist.org>).

Oligonucleotides

The right border of the *Atscc3-1* T-DNA was amplified by PCR with primers Stag1 (5'-GCAAGTTGGTTGCTAGTGATGTGG-3') and TAG3 (5'-CTGATACCAGACGTTGCCCGCATAA-3'); the left border was amplified with Stag2 (5'-CTTATCTTCTCTGTCTGACC-CGCC-3') and LbBar1 (5'-CAACCCTCAACTGGAAACGGGCC-GGA-3'). Wild-type *AtSCC3* was amplified with primers Stag1 and Stag2. For *Atscc3-2*, oligonucleotides ON521769-1 (5'-CAAAA-TCCAAATGCCAGAGAC-3') and ON521769-2 (5'-TCCAGAAA-GAAGGAACCAAGAAC-3') were used for the wild-type allele and ON521769-2 with LbSALK1 (5'-CATCAAACAGGATTTTCGCC-3') for the mutant allele. *AtREC8* and *AtSPO11-1* wild-type and mutant alleles were amplified as previously described (Bhatt et al., 1999; Grelon et al., 2001).

Genetic analyses

We tested for allelism between the two *Atscc3* mutations by crossing *Atscc3-1^{-/-}* (female) and *Atscc3-2^{-/-}* (male). Of the 117 F1 plants, 23 were *Atscc3-1^{+/-}*, 45 *Atscc3-2^{+/-}* and 49 were wild type for both loci. Thus, the two mutations are allelic and the heterozygous *Atscc3-1/Atscc3-2* is lethal.

Double mutants for *Atspo11-1-1* and *Atscc3-1* or *Atrec8* were obtained by crossing a plant heterozygous for the *Atspo11-1-1* mutation with plants heterozygous either for *Atscc3-1* or *Atrec8* mutations. The resulting hybrids were self-pollinated. We selected plants from the F2 progeny, segregating 15:1 for kanamycin resistance in vitro. We used PCR screening to select the sterile plants in the F2 progeny homozygous for both mutations.

Antibodies

The anti-ASY1 polyclonal antibody has been described elsewhere (Armstrong et al., 2002). It was used at a dilution of 1:500. The anti-REC8 polyclonal antibody (Cai et al., 2003) was used at a dilution of 1:250. The anti-RAD51 antibody (Anderson et al., 1997) was used at a dilution of 1:10.

The anti-SCC3 antibody was raised as follows: a 1442-bp DNA fragment was amplified from AY091270 corresponding clone (U11370) with the T3 promoter and LC1 (5'-GTGCCTCG-AGGATCAAGTGGTCATACA-3') primers; it was inserted into pTOPO2-1 (Invitrogen) and sequenced. An *NcoI-XhoI* fragment containing the DNA sequence encoding the first 417 amino acids of AtSCC3 was then subcloned in-frame into pET29a digested with *NcoI* and *XhoI* (Novagen). The resulting construct was transferred to *E. coli* BL21 cells (Novagen). Upon induction, the 452 amino acid recombinant protein accumulated in the insoluble fraction and was resolubilised in a binding buffer containing 5 M urea, 50 mM Tris-HCl, pH 8, 300 mM NaCl and 5 mM imidazol. The resulting suspension was subjected to ultracentrifugation at 100,000 g for 1 hour. The supernatant was incubated for 90 minutes

with 1 ml Ni-NTA Agarose (Qiagen) equilibrated in binding buffer. The resin was washed with 50 ml binding buffer and packed into an HR5/5 column connected to the Äkta Prime system (Amersham Biosciences). The protein was eluted using a gradient of imidazol (20–500 mM) and 0.3 ml fractions were collected at a rate of 0.3 ml/minute. Fractions containing AtSCC3 were pooled and the total amount of recombinant protein was determined with the Biorad Protein assay kit according to the manufacturer's instructions. Rabbit polyclonal antibodies were raised against the recombinant protein (Biogenes). The AtSCC3 antibody was used at 1:1000 dilution.

Microscopy

We observed the development of pollen mother cells by DIC microscopy, after clearing fresh buds of various sizes in Herr's buffer (phenol:chloral hydrate:85% lactic acid:xylene:clove oil; 1:1:1:0.5:1; v:v:v:v). We stained meiotic chromosomes with DAPI, as previously described (Ross et al., 1996).

Preparation of prophase stage spreads was performed as described (Armstrong et al., 2002) with the following modifications. For one slide, ten flower buds of the appropriate meiotic stage were used. Anthers were isolated from buds directly in 10 μ l enzyme digestion mixture (Armstrong et al., 2002). Then after adding another 10 μ l digestion mixture, anthers were incubated for 2 minutes at 37°C. After this time, anthers were tapped out using a hook, made with a cytological needle to release pollen mother cells (PMCs). To prepare the spreads, 10 μ l Lipsol spreading medium (1% Lipsol detergent in water buffered to pH 9.0 with borate buffer) was added to the droplet and incubated for 2 minutes at room temperature. During this time, the droplet was stirred with a hook. Then 20 μ l of 4% paraformaldehyde, pH 8.0 (Sigma) was added and the slide was allowed to dry. For immunolocalization, slides were washed in distilled water and immersed in PBS with 0.1% Triton X-100. For metaphase stages, spreads were performed as described (Ross et al., 1996), then treated in the microwave according to the method of Leong and Sormunen (Leong and Sormunen, 1998) before immunostaining. Fluorescence immunolocalization was performed according to published methods (Armstrong et al., 2002).

All observations were made using a Leica DM RXA2 microscope; photographs were taken using a CoolSNAP HQ (Roper) camera driven by Open LAB 3.1.5 software; all images were further processed with Open LAB 3.1.5 or Adobe Photoshop 7.0.

The mitotic index was determined as described (Hartung et al., 2002) on roots isolated from five wild-type plants and ten *Atsc3-1* plants grown for 21 days in the greenhouse.

Results

The *Arabidopsis* genome contains a single putative *Sc3* homologue

Blast searches (Altschul et al., 1990) with several *Sc3* proteins (*S. cerevisiae*, *M. musculus* Stag3 and *S. pombe* Rec11) revealed a single putative homologue among the *Arabidopsis* AGI proteins (<http://www.arabidopsis.org/Blast/>): At2g47980 (hereafter called AtSCC3). A cDNA clone corresponding to AtSCC3 was identified in the database (accession number AY091270). The protein encoded by AtSCC3 is 1098 amino acids long and is 21% identical and 40% similar to the ScSc3 protein (Blast2 sequence, Matrix Blossum 45) (Tatusova and Madden, 1999) (supplementary material Fig. S1B).

Using RT-PCR on mRNA from various tissues, we found that AtSCC3 was expressed equally strongly in roots, mature leaves, buds and plantlets (data not shown).

AtSCC3 is required for a normal vegetative development

We searched for *Atsc3* mutants in T-DNA insertion line collections. One mutant allele, *Atsc3-1*, was found to carry an insertion in exon 19 of AtSCC3 (supplementary material Fig. S1A,B). Sequencing of the DNA flanking the T-DNA in *Atsc3-1* showed that T-DNA insertion was accompanied by a deletion of 30 bp of exon 19 and the insertion of 14 bp of foreign DNA. This allele encodes a putative truncated protein consisting of the first 927 amino acids of AtSCC3 plus an additional seven amino acids at the C-terminus. A second insertion allele, *Atsc3-2*, has a T-DNA insertion at the boundary between intron 5 and exon 6 of AtSCC3 (supplementary material Fig. S1A,B). The *Atsc3-2* allele encodes a putative truncated protein containing only the first 193 amino acids encoded by AtSCC3. These two mutants were confirmed to be allelic by genetic tests (see Materials and Methods).

We investigated the effect of AtSCC3 disruption in plants by examining the progeny (self-fertilisation) of a heterozygous *Atsc3-2^{+/-}* plant. PCR genotyping of 115 plants from this progeny, using primers specific to the mutant or the wild-type allele, demonstrated the absence of homozygous mutant plants from this progeny (77 plants were heterozygous and 38 wild type), suggesting a defect in transmission of the mutant allele. Selfed *Atsc3-2^{+/-}* heterozygotes produced fewer seeds (22.9 \pm 1.9 seeds per silique, Fig. 1B) than did wild-type plants (54.4 \pm 3.6 seeds per silique, Fig. 1A) owing to the early abortion of some of the progeny. By analysing the transmission of the *Atsc3-2* allele to the progeny in backcrosses, we proved that *Atsc3-2* mutation was embryo-lethal (data not shown).

Sterile, dwarf plants were observed among the progeny of a heterozygous *Atsc3-1^{+/-}* plant (Fig. 1C,D,E). This phenotype segregated in a 3:1 ratio, indicating that the *Atsc3-1* mutation was monogenic and recessive. We genotyped 142 mutant plants and showed that all were homozygous for the mutant allele *Atsc3-1*, demonstrating strong linkage between AtSCC3 disruption and the mutant phenotype. We investigated the phenotype of *Atsc3-1* mutants on synthetic medium and in soil. Mutant organs were smaller than those of wild-type plants by a factor of two to five (Table 1) under all conditions tested. We also analysed the proportion of dividing cells in root tips. Mutant roots contained only one-third as many dividing cells as wild-type roots (Table 1).

These data indicate that AtSCC3 disruption is lethal and that a leaky mutation (*Atsc3-1*) greatly disturbs plant development and may be correlated with mitotic defects.

Meiosis is impaired in *Atsc3-1* mutants

The fertility of *Atsc3-1* plants was extremely low, with only very small numbers of seeds produced (Table 1). We therefore examined the reproductive development of this mutant, and found that the sterility of *Atsc3-1* mutants was correlated with abortion of the male and female gametophytes (data not shown). With the aim of identifying the stages of sporogenesis and/or gametogenesis impaired in *Atsc3-1*, we examined developing male gametophytes by DIC microscopy of cleared buds.

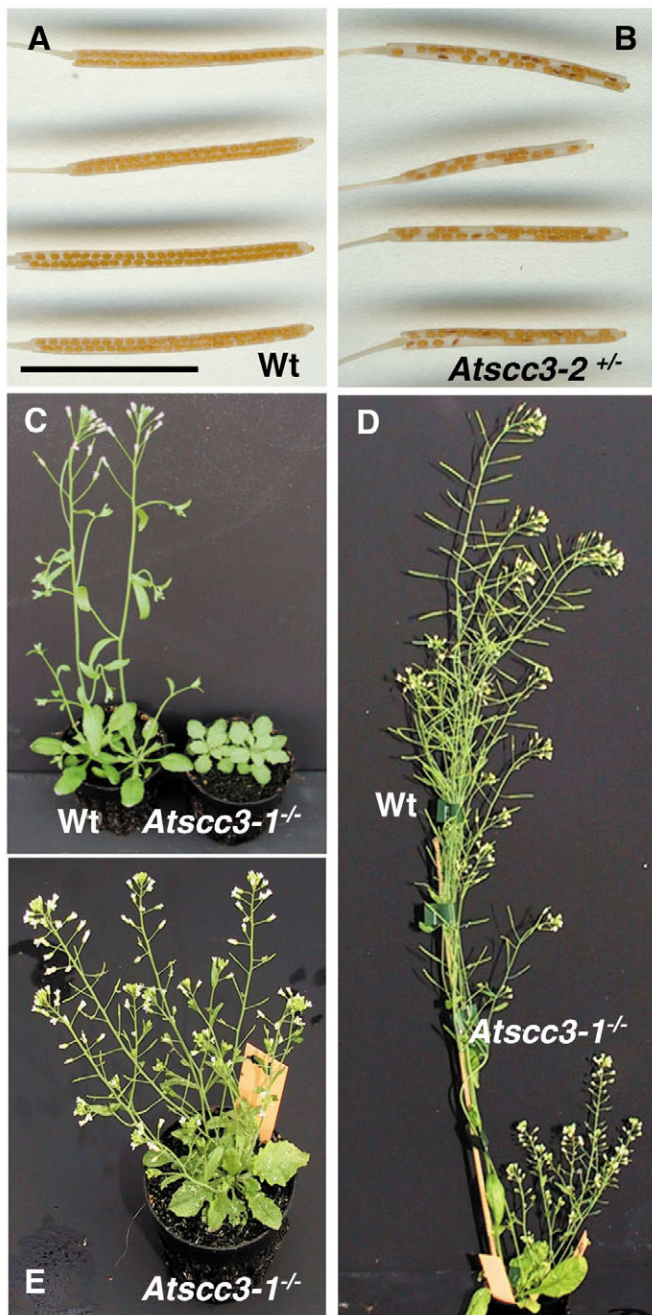
Comparison of the early stages of microsporogenesis revealed no difference between wild-type and mutant plants (Fig. 2A,C): round pollen mother cells (PMCs) were

Table 1. *Atscc3-1* phenotype

		Wild type	<i>Atscc3-1^{+/-}</i>	<i>Atscc3-1^{-/-}</i>	Ratio*
First leaf area (mm ²)	21 days, greenhouse	24.5±6.5 (n=5)	n.d.	7.9±0.9 (n=7)	3
Rosette diameter (mm)	21 days, greenhouse	33.3±7.2 (n=19)	30.5±7.9 (n=52)	14.7±2.9 (n=42)	2.3
Floral scape size (mm)	37 days, greenhouse	274±35 (n=16)	240±85 (n=45)	52±26 (n=42)	5
Primary root size (mm)	10 days, in vitro	48.7±6.9 (n=40)	47.9±6.3 (n=55)	14.5±2.9 (n=45)	3.3
Root apex mitotic index		23/1000 (n=5036)	n.d.	7/1000 (n=9916)	3.3
Fertility (no. seeds/silique)	Greenhouse	43.4±6.9 (n=95)	45.5±5.2 (n=93)	0.1±0.1 (n=27)	–

Several aspects of *Atscc3-1* mutant development (leaves, rosette, floral scape and primary root) were studied and compared with those of the wild type and heterozygotes (*Atscc3-1^{+/-}*) grown in identical conditions (in vitro or in the greenhouse). Mitotic index was defined as the number of metaphase, anaphase and telophase nuclei identified, divided by the total number of nuclei observed; fertility was estimated as the number of seeds produced per silique. *n* is the number of plants for which measurements were made, except for mitotic index, where *n* indicates the number of cells counted, and fertility, where *n* is the number of siliques observed.

*This ratio was obtained by dividing the wild-type value by the mutant value (*Atscc3-1^{-/-}*).
n.d., not determined.



distinguished within the anther locules. In wild-type anthers, these cells underwent two meiotic divisions to produce a characteristic tetrad of microspores enclosed in a callose wall (Fig. 2B). Meiosis products were also detected in mutant plants, but lacked the regular tetrahedral structure, and were either asymmetric tetrads or ‘polyads’ containing more than four products (Fig. 2D), suggesting disturbance of the meiotic program in *Atscc3-1*.

We therefore investigated male meiosis in *Atscc3-1* plants by staining chromosomes with 4',6-diamidino-2-phenylindole (DAPI). Wild-type *Arabidopsis* meiosis has been described in detail (Ross et al., 1996), and the major stages are summarised here (Fig. 2E-I). During prophase I, meiotic chromosomes condense, recombine and undergo synapsis, resulting in the formation of five bivalents, each consisting of two homologous chromosomes attached to each other by sister chromatid cohesion and chiasmata, which become visible at diakinesis (Fig. 2F). Synapsis, the close association of two chromosomes via a synaptonemal complex (SC), begins at zygotene and is complete by pachytene, by which point the SC has polymerised along the length of the bivalents (Fig. 2E). At metaphase I, the five bivalents are easily distinguishable (Fig. 2G). During anaphase I, each chromosome separates from its homologue (Fig. 2H), leading to the formation of dyads corresponding to two pools of five chromosomes (not shown). The second meiotic division then separates the sister chromatids, generating four pools of five chromosomes (Fig. 2I), which give rise to tetrads of microspores (Fig. 2B). Chromosome condensation and synapsis occurred in *Atscc3-1* PMCs (Fig. 2J,O). Nevertheless, fully synapsed chromosomes were rarely observed: among 118 cells at zygotene or pachytene stages in *Atscc3-1*, only 11 displayed full synapsis (9%), whereas among 91 wild-type PMCs at the same stages, 43 were found to be fully synapsed pachytene (47%). Further examination of pachytene-like stages in the mutant revealed an abnormal (fluffy) appearance of the chromatin. Condensation abnormalities were observed in pericentromeric heterochromatin, which was abnormally rounded in the mutant (compare Fig. 2E,J,O, asterisks). Nevertheless, condensation and progression through the

Fig. 1. *Atscc3* mutant phenotypes. (A,B) Siliques from wild-type (A) or heterozygous *Atscc3-2^{+/-}* plants after clearing. (C-E) Comparison of wild-type (Wt) and homozygous mutant *Atscc3-1^{-/-}* plants after 21 days (C) or 40 days (D,E) in the greenhouse. Bar, 1 cm.

subsequent stages of meiosis occurred in *Atscc3-1* PMCs. At diakinesis and metaphase I (Fig. 2K,P,L,Q), a complex combination of bivalents and univalents was observed, with these structures often tangled. At anaphase I, we observed 15 to 20 chromosomes segregating toward the poles (Fig. 2M,R), suggesting the premature separation of sister chromatids at the first meiotic division. In some cells (9 of 85), we also detected chromosome fragmentation (Fig. 2R, arrows). Occasionally we also observed chromosomes that failed to separate their chromatids leading to the formation of chromatin bridges (Fig. 2M, arrows). At the second meiotic division, we observed random segregation of the separated chromatids, giving rise to variable numbers of daughter cells with different numbers of chromosomes. In some cases, we observed chromosome bridges that could correspond either to chromatids subjected to bipolar tension or to univalents that fail to separate their sister chromatids (Fig. 2N,S). An analysis of female meiosis in *Atscc3-1* identified defects similar to those seen during male meiosis (data not shown). Thus, *AtSCC3* is involved in both male and female meiosis and its disruption provokes an early release of cohesion at anaphase I.

AtSCC3 is located on chromosome axes during meiosis, until anaphase I and is present throughout the mitotic cycle

We investigated the function of AtSCC3 during meiosis with the aid of antibodies against the N-terminal sequence of the protein. We co-immunolocalised AtSCC3 and ASY1, a protein associated with the axial element of meiotic chromosomes (Armstrong et al., 2002), and compared the two signals.

AtSCC3 immunolocalisation revealed a strong signal in the nuclei of wild-type PMC from meiotic interphase up to and including metaphase I (Fig. 3). During interphase, AtSCC3 was detected as foci in the nucleus (Fig. 3B,E). As the chromosomes condensed during leptotene, the AtSCC3 signal appeared on chromatin, delineating the chromosome axis. At this stage, staining with anti-SCC3 antibody was consistently more punctate than the linear staining of the chromosome axis observed with anti-ASY1 antibody (Fig. 3J,K). By zygotene and pachytene, AtSCC3 and ASY1 signals overlapped showing that at this stage chromosome axes were stained with AtSCC3 (Fig. 3M,N). At diplotene and diakinesis the signal weakened, but could still be observed on the chromosome axis (Fig. 3Q). At metaphase I, only the arms of each bivalent were stained with anti-SCC3 serum (Fig. 3T,W). Although the signal was faint and often punctate at this stage, the anti-SCC3 serum clearly

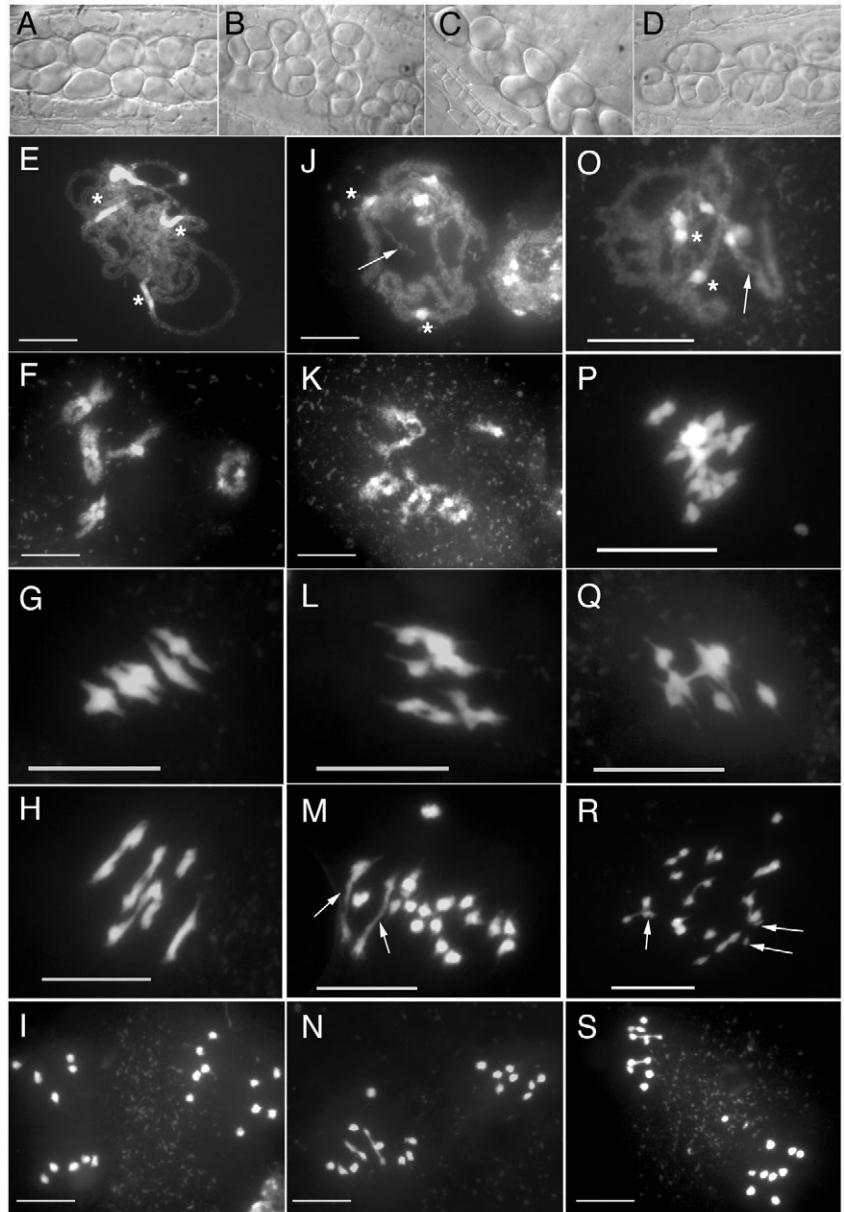


Fig. 2. Male sporogenesis and meiosis of wild-type (A,B,E-I) and the *Atscc3-1* mutant (C,D,J-S). (A,D) DIC microscopy of male meiocytes (A,C) and of the products of male meiosis (tetrads of microspores, B and D). (E-S) DAPI staining of wild-type and mutant pollen mother cells during meiosis. (E) Pachytene, (F) diakinesis, (G) metaphase I, (H) anaphase I, and (I) end of anaphase II in wild-type meiocytes. The same stages are shown in *Atscc3-1* mutant pollen mother cells: (J,O) pachytene, (K) diakinesis, (P,L,Q) metaphase I, (M,R) anaphase I and (N,S) anaphase II. Asterisks indicate pericentromeric heterochromatin during pachytene stages (E,J,O). Arrows indicate some of the abnormalities observed in the *Atscc3-1* mutant: synapsis defects at pachytene (J,O), chromosome bridges (M) and chromosome fragmentation (R). Bar, 10 μ m.

delineated the two homologous arms of the bivalent (Fig. 3W,X, arrows). No signal corresponding to AtSCC3 was detected in centromeric regions during metaphase I, anaphase I or metaphase II (data not shown). ASY1 and AtSCC3 were colocalised at most meiotic stages, except metaphase, during which no ASY1 was detected, and in very young meiocytes,

in which ASY1 was barely detectable, whereas AtSCC3 was detected (Fig. 3A,B). This suggested that AtSCC3 was present in meiotic nuclei before ASY1, probably in G1.

A weak signal was obtained with the anti-SCC3 antibody in *Atsc3-1* pollen mother cells, confirming the leaky expression of AtSCC3 in *Atsc3-1* mutants. However, when AtSCC3 signal was detected (7 out of 18 cells), it was either very faint or associated with the nucleolus (4 out of 7 cells) or forming patches in the nucleus but not on the chromatin of *Atsc3-1* plants, suggesting that *Atsc3-1* plants produce a truncated version of AtSCC3 that accumulates at low levels and displays an aberrant distribution (Fig. 3Z,AC). However, ASY1 staining was perfectly normal in the *Atsc3-1* mutant background (Fig. 3Y,AB, but also Fig. 4I,M).

The staining of vegetative nuclei with anti-SCC3 serum (Fig. 3AF and supplementary material Fig. S2) confirmed the involvement of AtSCC3 in both meiosis and mitosis, in contrast to that observed for ASY1 (Fig. 3AE). AtSCC3 was detected throughout the mitotic cell cycle during interphase (G1, S, G2, supplementary material Fig. S2C-L) as well as on the chromosome axis as the chromosomes condense (supplementary material Fig. S2A,B).

Is AtSCC3 involved in meiotic recombination?

As the *Atsc3-1* mutant displayed a mix of univalents and bivalents at metaphase I, we wondered whether recombination was occurring at normal levels in the mutant background. We analysed the nuclear distribution of the protein RAD51, which is an essential component of the recombination machinery. Its appearance on meiotic chromosomes during prophase is thought to reflect the progression of recombination repair (Masson and West, 2001). RAD51 staining of meiotic chromosomes has been described in several plant species: maize (Franklin et al., 1999), *Lilium* (Terasawa et al., 1995) and *Arabidopsis* (Mercier et al., 2003). We used an antiserum directed against tomato RAD51 and obtained results similar to those for other species. RAD51 foci appeared at leptotene, were most abundant at zygotene (Fig. 4A-H), and tended to disappear during pachytene (not shown). A similar pattern of RAD51 staining was observed in *Atsc3-1* pollen mother cells (Fig. 4I-P). Quantification of this staining at zygotene stages showed that approximately the same number of foci were present in both genotypes (222 ± 59 , $n=10$ for *Atsc3-1* cells; 210 ± 23 , $n=7$ in wild-type cells). Therefore, the number of recombination initiation sites is unlikely to be much lower in *Atsc3-1* cells than in the wild type.

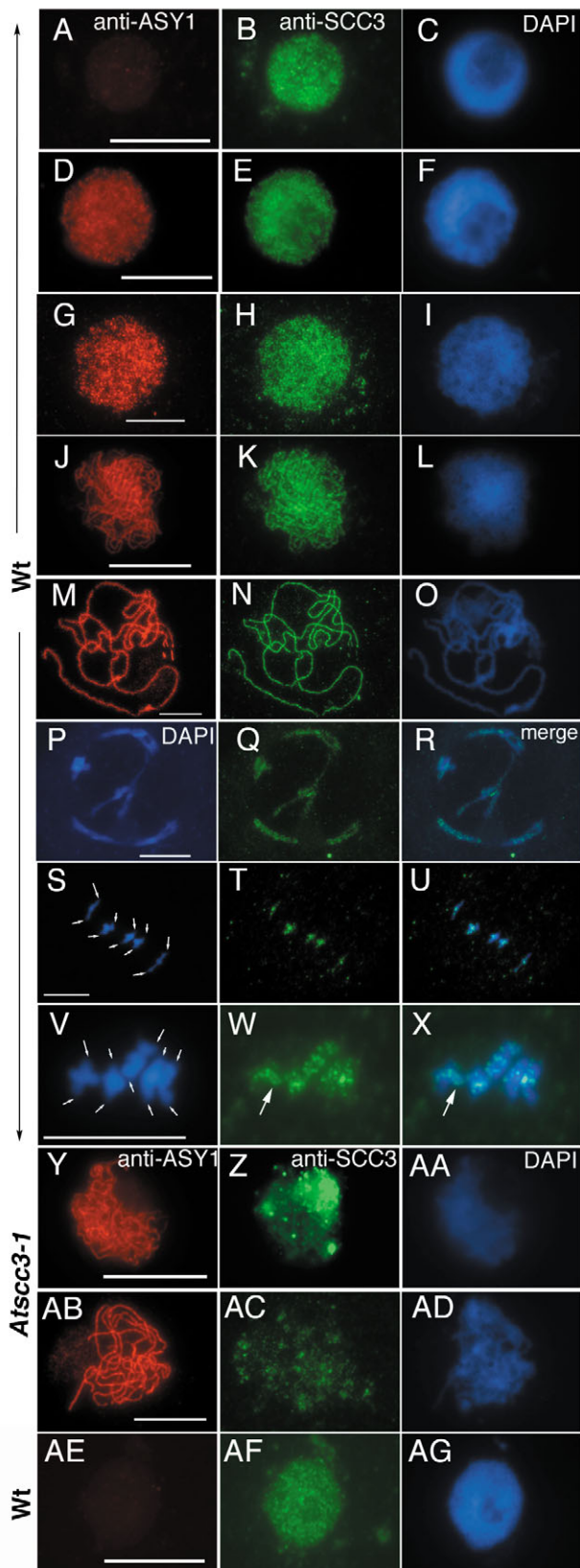


Fig. 3. Immunolocalisation of ASY1 and AtSCC3 in wild-type and *Atsc3-1* mutant cells. (A-AD) Male meiotic cells. (AE-AG) A wild-type vegetative cell, easily distinguishable from meiocytes based on its size and small nucleolus. (A,B,C) Early interphase meiocyte, probably in G1 as ASY1 labelling is very faint. (D,E,F) Interphase meiocyte, probably in G2 according to ASY1 staining, which is strong. (G,H,I) Leptotene; (J,K,L) zygotene; (M,N,O) pachytene; (P,Q,R) diakinesis; (S-X) metaphase I; (Y-AA) zygotene; (AB-AD) pachytene. Arrows in S and V indicate centromeres, and arrows in W and X indicate the AtSCC3 staining corresponding to chromosome arms. For each cell, several stains are shown: anti-ASY1 (in red), anti-SCC3 (in green), and in blue, the DAPI staining of chromatin (DAPI). For diakinesis and metaphase I cells, no ASY1 staining is shown, but an overlay of DAPI and AtSCC3 staining is shown (merge). Bar, 10 μ m.

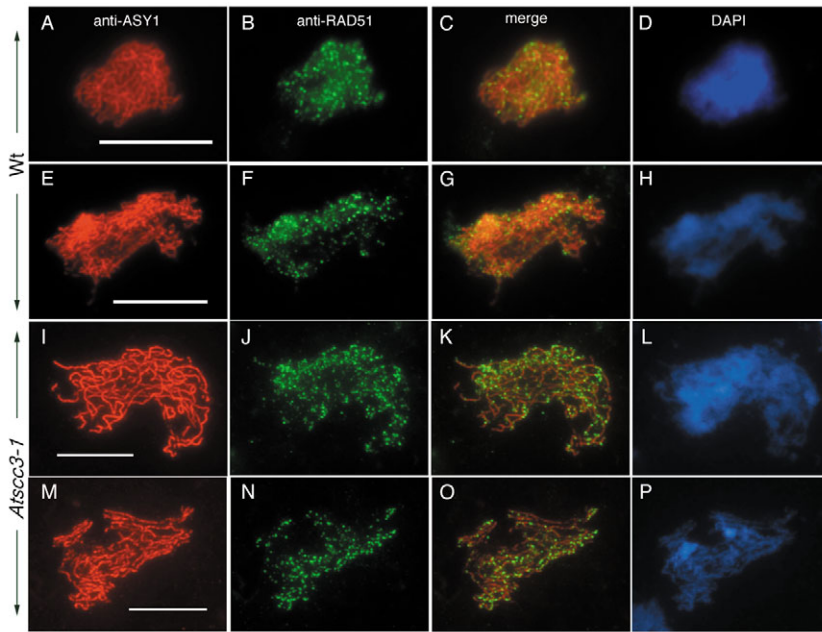


Fig. 4. Immunolocalisation of ASY1 and RAD51 in wild-type and *Atsc3-1* pollen mother cells. (A–H) Wild-type cells (Wt). (I–P) *Atsc3-1* mutant cells. An overlay of the two signals is shown (merge), together with DAPI staining of the corresponding cell (DAPI). Bar, 10 μ m.

AtREC8 and AtSCC3 are necessary, but not sufficient, for the monopolar orientation of the kinetochores during meiosis I

DIF1/SYN1 (hereafter AtREC8), another member of the cohesin complex in *Arabidopsis*, is thought to be the *Arabidopsis* Rec8 homologue (Bai et al., 1999; Bhatt et al., 1999; Cai et al., 2003). In *Atrec8* mutants, PMCs display multiple meiotic defects and univalents and chromosome fragmentation is observed at metaphase I (Bai et al., 1999; Bhatt et al., 1999) (Fig. 5E). Chromosome fragmentation and chromatin bridges were evident at anaphase I (Fig. 5F; observed in 28 cells out of 36; 77%), leading previous investigators to suggest that *Atrec8* was defective in recombination repair (Bai et al., 1999; Bhatt et al., 1999). In order to check this hypothesis and to compare AtREC8 with AtSCC3, we introduced the *Atspo11-1-1* mutation (Grelon et al., 2001) into the *Atrec8* and *Atsc3-1* mutant backgrounds. In *Atspo11-1-1* mutants, the dramatic decrease in the formation of double-strand breaks (DSB) prevents recombination, resulting in univalents being observed at metaphase I, rather than bivalents (Grelon et al., 2001) (Fig. 5C). These univalents segregate randomly at meiosis I (Fig. 5D), and sister chromatid segregation does not occur before meiosis II (not shown). When the *Atspo11-1-1* mutation was introduced into *Atrec8* or *Atsc3-1* mutants, PMCs at meiosis I also had ten univalents (Fig. 5I,K), and no more chromosome fragmentation was observed. At anaphase I, the univalents of both double mutants, *Atspo11-1-1Atsc3-1* and *Atspo11-1-1Atrec8*, underwent a mitosis-like division, with separation of the sister chromatids of all univalents (Fig. 5J,L) but reductional division was never observed ($n=44$ for *Atspo11-1-1Atsc3-1* and $n=19$ for *Atspo11-1-1Atrec8*). In both cases this first equational division was followed by random segregation of the chromatids at

meiosis II (not shown). Thus, in both *Atsc3-1* and *Atrec8* mutants, centromere cohesion is maintained through prophase but lost at anaphase I, and sister kinetochores have a bipolar rather than a monopolar orientation, transforming the first meiotic division into a mitotic one.

AtSCC3 localisation on chromosomes depends on AtREC8

We investigated the effect of disrupting one cohesin on the location of its putative partner. The antibodies against AtREC8 used here have been described elsewhere, and AtREC8 has been detected on chromosome arms from meiotic interphase to anaphase I (Cai et al., 2003) (Fig. 6B). The distribution of AtREC8 was similar in *Atsc3-1* and wild-type PMCs (Fig. 6E,H). By contrast, when we incubated anti-SCC3 antibody with *Atrec8* meiocytes, we detected AtSCC3 in young meiocytes (interphase, Fig. 6K) but not at subsequent meiotic stages (Fig. 6N,Q). This suggests that AtREC8 is required for the correct binding of AtSCC3 to meiotic chromosome axes or for stabilisation of that binding.

AtREC8 is necessary for correct chromosome axis structure, independently of AtSPO11-1-induced DSBs

We observed that the ASY1 signal in *Atsc3-1* PMC (Fig. 6D,G and Fig. 3Y,AB) was the same as that of the wild type (Fig. 3A,D,G,J,M and Fig. 6A). However, the distribution of ASY1 was strongly abnormal in *Atrec8* PMC (Fig. 6M,P), with most of these cells showing only short stretches of ASY1 staining in *Atrec8*. These results suggest that a normal chromosome axis develops in *Atsc3-1*, but not in *Atrec8* mutants. We investigated whether this axis abnormality was a consequence of the chromosome fragmentation observed in the *Atrec8* mutant by analysing the distribution of ASY1 in the *Atspo11-1-1Atrec8* double mutant, which lacks SPO11-induced DSBs and displays no chromosome fragmentation (see above). We found that even in the absence of chromosome fragmentation, ASY1 was distributed unevenly, in short stretches, in *Atspo11-1-1Atrec8* PMCs (Fig. 7A,D), indicating that the axis defect of the *Atrec8* mutant was independent of DSBs.

AtSPO11-1 plays a role in the stabilisation of the cohesin complex when AtSCC3 is mutated

When we analysed the distribution of ASY1 and AtREC8 in the *Atspo11-1-1Atsc3-1* double mutant, young meiocyte nuclei were labelled by both ASY1- and AtREC8-specific antibodies (Fig. 7G,H), but the AtREC8 signal was difficult to detect once axis formation was complete and at subsequent meiotic stages (Fig. 7K,N,Q). When we analysed the ASY1, AtSCC3 and AtREC8 staining in the *Atspo11-1-1* single mutant, we found that their distributions were more similar to that seen in the wild type (Fig. 7S–Z'), suggesting that AtREC8

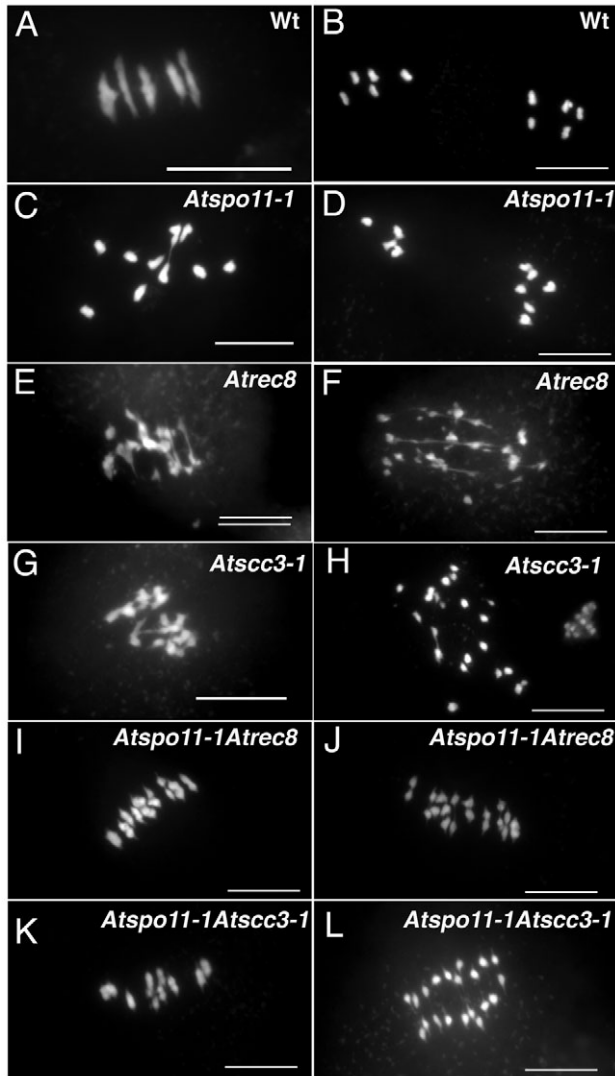


Fig. 5. DAPI staining of male meiocytes at metaphase-anaphase transition and during anaphase I. Several genotypes are shown: wild-type (Wt) (A,B), *Atspo11-1-1* (C,D), *Atrec8* (E,F), *Atscc3-1* (G,H), double mutants *Atspo11-1-1Atrec8* (I-J) and *Atspo11-1-1Atscc3-1* (K,L) at metaphase-anaphase transition (left-hand column) and during anaphase I (right-hand column). Bar, 10 μ m.

stabilisation or correct association with chromosomes needs the presence of both AtSCC3 and AtSPO11-1.

Discussion

Identification of the *Arabidopsis* Scc3 cohesin

Of all the subunits of the cohesin complex, we know the least about the role of Scc3 during mitosis and meiosis. In both *S. cerevisiae* and *C. elegans* *scc3* mutants, cohesion is lost before anaphase I, leading to extensive missegregation (Toth et al., 1999; Pasierbek et al., 2003; Wang et al., 2003). In *S. pombe*, which has two *Scc3* homologues, the ubiquitous *Psc3* and the meiosis-specific *Rec11*; *Rec11* is located primarily on chromosome arms, whereas *Psc3* is localised at the centromere, defining distinct chromosomal regions (Kitajima et al., 2003). Here we report the identification and functional analysis of

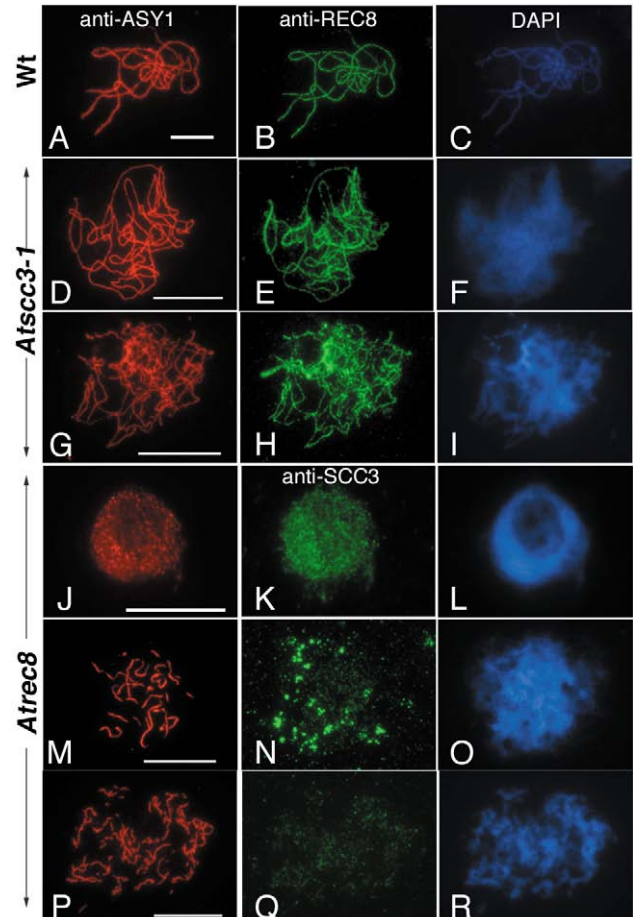


Fig. 6. Immunolocalisation of ASY1, AtSCC3 or AtREC8 in meiocytes from wild-type (Wt), *Atscc3-1* and *Atrec8* plants. ASY1 (anti-ASY1) in red, and in green either AtREC8 (anti-REC8) or AtSCC3 (anti-SCC3). DAPI staining of chromatin (DAPI) is blue. Bar, 10 μ m.

the sole *Scc3* gene in the *Arabidopsis* genome. Several of our results suggest that AtSCC3 is a mitotic cohesin: first, AtSCC3 is ubiquitously expressed in all tissues undergoing cell division; second, the embryo lethality of the *Atscc3-2* null allele and the mitotic defects of the leaky *Atscc3-1* allele, all indicate involvement in mitosis. We also found that AtSCC3 was involved in meiosis, as we detected AtSCC3 in meiotic nuclei as early as interphase, bound to the chromosome axis from early leptotene through to anaphase I. The AtSCC3 localisation pattern during meiosis is very similar to that for AtREC8 (Cai et al., 2003), which, at least in yeasts, has been shown to be the meiotic partner of Scc3 (Toth et al., 1999; Kitajima et al., 2003). In addition, the meiotic phenotype of the *Atscc3-1* mutant confirmed the involvement of AtSCC3 in meiotic sister chromatid cohesion.

AtSCC3 and AtREC8 are necessary for the maintenance of centromeric cohesion at meiotic anaphase I

In all models used in the study of meiosis, the cohesin Scc1 is mostly replaced by its meiotic equivalent, Rec8, allowing the

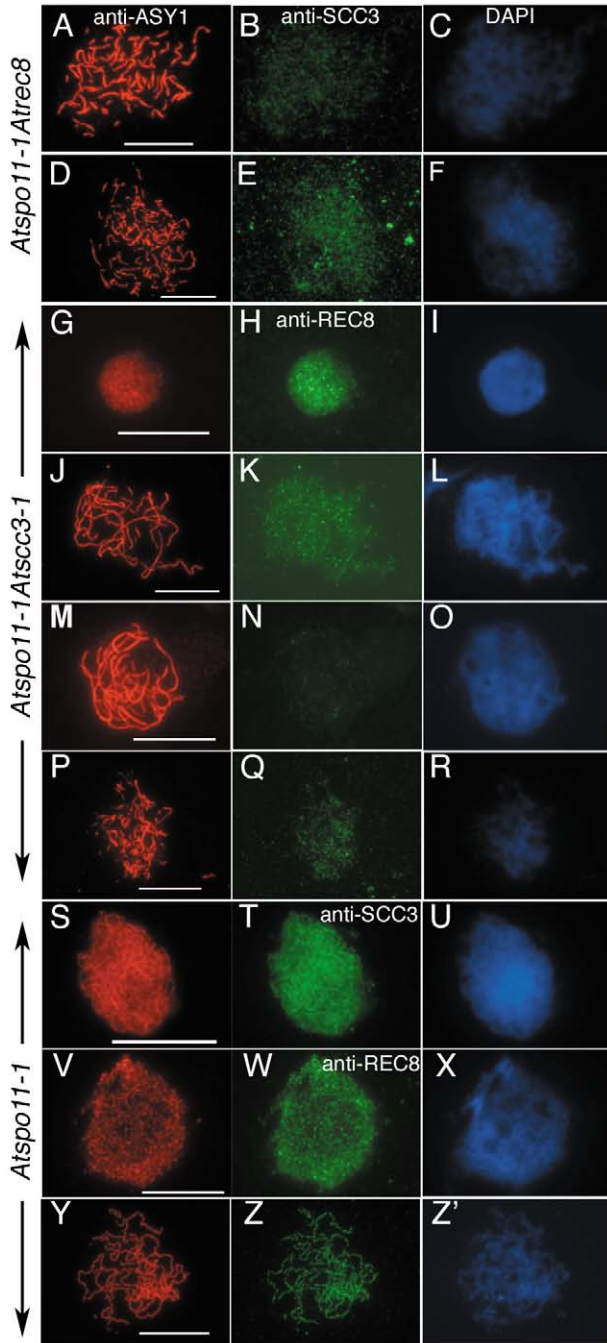


Fig. 7. Immunolocalisation of ASY1, AtSCC3 or AtREC8 in meiotic cells from double mutants *Atspo11-1-Atrec8*, *Atspo11-1-Atsc3-1* or single *Atspo11-1-1* mutant plants. In red, immunolocalisation of ASY1 (anti-ASY1); in green, immunolocalisation of AtREC8 (anti-REC8) or AtSCC3 (anti-SCC3); and in blue, the DAPI staining of chromatin (DAPI). Bar, 10 μ m.

cohesin complexes to fulfil their meiotic functions. During the anaphase of the first meiotic division, the dissociation of Rec8 from the chromosome arms releases arm cohesion, allowing homologous chromosomes to segregate, whereas centromeric cohesion is maintained until anaphase II owing to the protection of Rec8 from cleavage by Sgo1, recently isolated in

S. cerevisiae and *S. pombe* (Katis et al., 2004; Kitajima et al., 2004; Marston et al., 2004; Rabitsch et al., 2003). In this report, we show that chromosomes in *Atsc3-1*, *Atspo11-1-Atrec8* and *Atspo11-1-Atsc3-1* mutants separate their sister chromatids at anaphase I. This indicates that in *Arabidopsis*, both AtREC8 and AtSCC3 are absolutely necessary for the maintenance of cohesion at centromeres in anaphase I. Interestingly, centromere cohesion was not lost until anaphase I, either in the *Atsc3-1* or in *Atrec8* mutants, suggesting that neither of these proteins is absolutely necessary for cohesion until this stage. This is in contrast to that found for these cohesins in *C. elegans* (Pasierbek et al., 2001; Pasierbek et al., 2003; Wang et al., 2003), *S. cerevisiae* (Klein et al., 1999) but similar to *S. pombe rec8 phenotype or mouse *rec8* mutant (Watanabe and Nurse, 1999; Xu et al., 2005). In *S. pombe rec8* mutants, Rad21 (the Scc1 homologue) was found to relocate to centromeres and consequently maintained centromeric cohesion until separase action at anaphase I (Yokobayashi et al., 2003). Moreover, the localization of Rad21 in meiotic prophase cells has also been shown in mouse (Parra et al., 2004), suggesting its involvement in meiotic cohesion in other organisms as in fission yeast. As the *Arabidopsis* genome contains three other Scc1-like sequences (Dong et al., 2001), we hypothesize that one of these Scc1 homologues probably behaves in a similar manner in the *Atrec8* background, and maintains cohesion until anaphase I. The situation of *Atsc3-1* is more striking as there are no additional Scc3 homologues identifiable in the *Arabidopsis* genome that could partially compensate for the loss of AtSCC3. We cannot exclude the possibility that the small amount of the truncated protein still present in the *Atsc3-1* mutant may function with Scc1 to maintain cohesion during these early stages but is not protected at anaphase I. Alternatively, a non-cohesin mechanism may function in sister chromatid cohesion during the early stages of meiosis. In this regard, it should be noted that Scc1-dependent cohesion is not protected during anaphase I, as has been demonstrated in both budding and fission yeast (Watanabe, 2004). In plants, a specific mutation in *Switch1* (encoding a protein involved in the establishment of sister chromatid cohesion during S phase) leads to a loss of cohesion only during late prophase (Mercier et al., 2003; Mercier et al., 2001). Specific antibodies raised against AtREC8 and AtSCC3 do not stain the centromeres after prometaphase, despite their involvement in centromere function (Cai et al., 2003) (this study). Indeed, many studies have reported a failure of antibodies against cohesins in general (Cai et al., 2003; Losada et al., 1998; Waizenegger et al., 2000) and against SCC3 in particular (Pasierbek et al., 2003) to detect their antigens on metaphase chromosomes despite the clear involvement of these proteins in centromeric cohesion. Thus the inability to detect AtREC8 and AtSCC3 on meiotic centromeres after prometaphase is neither unprecedented nor is it unusual, suggesting that the structure of the centromere at this stage prevents the antibodies from accessing their target.*

AtSCC3 and AtREC8 are necessary to the monopolar orientation of the kinetochores during meiosis I

During meiosis I, sister kinetochores are mono-orientated, allowing the attachment of the two sisters by microtubules emanating from the same pole. In *S. cerevisiae*, a protein

complex (the monopolin) is necessary for establishing this monopolar attachment (Toth et al., 2000; Rabitsch et al., 2003), but Rec8 does not play such a critical role in this process, as expression of the mitotic cohesin *Sccl* by the *Rec8* promoter can also provide monopolar orientation at metaphase I (Toth et al., 2000). It is not clear yet if this situation is conserved among species because the monopolin complex has not yet been described in any other organism and because in *S. pombe*, in contrast to *S. cerevisiae*, Rec8 was shown to be necessary for monopolar orientation of the kinetochores (Watanabe and Nurse, 1999; Yokobayashi et al., 2003). The phenotype of *rec8* mutants in other species was less informative because either cohesion was lost prematurely (before metaphase) as in *S. cerevisiae* (Klein et al., 1999), or *rec8* depletion provokes apoptosis as in mammals (Bannister et al., 2004) or strong chromosome fragmentation as in *Arabidopsis* (Bai et al., 1999; Bhatt et al., 1999) (this study). We abolished this chromosomal fragmentation by introducing the *Atspo11-1-1* mutation into the *Atrec8* background, leading to the production of ten univalents. As these univalents align correctly on a metaphase plate and are submitted to a bipolar tension leading to a mitotic-like division, it demonstrates that in *Arabidopsis*, as in *S. pombe*, *AtREC8* disruption leads to a bipolar orientation of the kinetochores. We observe that *AtSCC3* depletion induces exactly the same bipolar kinetochores as *AtREC8* depletion. This suggests that either *AtREC8* per se is not sufficient for the monopolar orientation of the kinetochores, or that it may be rendered inactive in the absence of the other members of the cohesin complex as *AtSCC3*. Further investigation on the effect that *AtSCC3* depletion has on other cohesins at the centromeres could reveal more about the mechanisms regulating kinetochore orientation.

Do AtREC8 and AtSCC3 play different roles in the cohesin complex during meiosis?

Sccl interacts directly with *Scc1* in the cohesin complex in yeast mitosis (Toth et al., 1999), *Xenopus* oocytes and human cell lines (Losada et al., 2000). In *S. pombe* meiosis, the two *Sccl* homologues, *Psc3* and *Rec11*, interact with *Rec8* (Kitajima et al., 2003) and in *C. elegans*, *SCC-3* and *REC-8* seem to control each other's location on the chromosome (Pasierbek et al., 2003). We provide evidence here that both *AtREC8* and *AtSCC3* are required for monopolar kinetochore orientation and for the maintenance of centromere cohesion at anaphase I, suggesting that they too are part of the same complex in meiosis. However, our data also suggest that these two cohesins display some specificity in their function, in particular they differ in their involvement in meiotic DSB repair.

In addition to its mechanistic role during cell division, cohesion between sister chromatids seems to be required for efficient DSB repair during the mitotic and meiotic cell cycles. Many cohesin mutants are sensitive to radiation and/or defective in DSB repair during the vegetative cell cycle (van Heemst and Heyting, 2000). Meiotic recombination is initiated by DSB formation, induced by Spo11 (for a review, see Keeney, 2001). The *rec8* and *smc3* mutants of *S. cerevisiae*, and *C. elegans* and *Arabidopsis rec8* mutants accumulate broken chromosomes during meiosis which are thought to reflect defects in recombination repair (Bai et al., 1999; Bhatt

et al., 1999; Klein et al., 1999; Bai et al., 1999; Bhatt et al., 1999; Klein et al., 1999; Pasierbek et al., 2001). It has also been shown that *rec8* and *rec11* mutations in *S. pombe* reduce meiotic recombination, whereas mutations in *psc3* do not (DeVeaux and Smith, 1994; Kitajima et al., 2003; Krawchuk and Wahls, 1999). In mammals, a meiotic variant of *Smc1* (*SMC1 β*) is required for chiasma formation, but not for the early steps of meiotic recombination (Revenkova et al., 2004). Cohesion (or cohesins) is therefore necessary for meiotic recombination, probably for the repair of meiotic DSBs, but the mechanism by which these processes are linked remains largely unknown. We confirmed the role of *AtREC8* in meiotic DSB repair showing that *Atrec8* fragmentation is abolished in an *Atspo11-1-1* mutant background. In the *Atsc3-1* mutant, we detected only a low level of fragmentation (in only 10% of the cells compared to 77% of *Atrec8* cells). This low level of fragmentation was probably not due to a large decrease in recombination initiation because RAD51 foci were formed normally; almost normal synapsis was observed at pachytene; and bivalents were formed in the *Atsc3-1* mutant. Therefore, *AtSCC3*, unlike *AtREC8*, might not be a key player in meiotic DSB repair in *Arabidopsis*.

We also showed that *AtREC8* is a key player in chromosome axis structure during meiosis because ASY1 staining highlighted a fragmented and split axis in the *Atrec8* mutant. This is consistent with *REC8* providing the basis for AE assembly (Eijpe et al., 2003) and with the involvement of *REC8* in axis structure, as has been shown in various organisms (Klein et al., 1999; Eijpe et al., 2000; Molnar et al., 2003). We also show that these axis defects are independent of Spo11-induced DSBs, because axis structure was not rescued in *Arabidopsis Atspo11-1-1Atrec8* double mutants. The ASY1 axis appeared perfectly normal in *Atsc3-1* mutants, suggesting that in contrast to *AtREC8*, *AtSCC3* might not be involved in this process.

Of course we cannot exclude the fact that these differences between *Atrec8* and *Atsc3-1* can be explained by the leaky nature of *Atsc3-1* mutation even if *Atsc3-1* and the double mutant, *Atspo11-1-1Atsc3-1*, display a fully penetrant phenotype for centromeric cohesion and kinetochore orientation (see above), and for *AtREC8* absence of labelling in *Atspo11-1-1Atsc3-1* (Fig. 7). Further investigations with a specific meiotic RNAi extinction of *AtSCC3* would help to answer this question. The functions of *Sccl* and *Scc3* have already been uncoupled in *Drosophila* mitotic cells, where depletion of *Sccl* (*Drad21*) or *Scc3* (*SA1*) homologues resulted in a different phenotype, even though there are no other homologues of these proteins in *Drosophila* (Vass et al., 2003). Therefore, although *Rec8* and *Scc3* are likely to be part of the same complex, these cohesins may also act independently to fulfil additional functions, through specific interaction with various proteins (recombination, axis building, etc.).

AtSPO11-1 is required for the stabilisation of sister chromatid cohesion in meiosis when *AtSCC3* is mutated. Cohesin behaviour was strongly modified by the introduction of the *Atspo11-1-1* mutation into the *Atsc3-1* mutant (compare Figs 6 and 7). Although *AtREC8* was present in normal amounts during meiotic interphase in the double mutant, it was barely detectable at later stages (Fig. 7). The presence of

AtREC8 at meiotic interphase shows that the protein is normally imported into the nuclei. Although it was not possible to determine at this stage whether AtREC8 was associated with chromatin, the *Atspo11-1-Atscc3-1* double mutant formed perfectly normal axial elements (AE) (according to ASY1 staining, Fig. 7), indicating that its disappearance at later stages resulted from dissociation from the chromatin rather than a loading defect. Our results clearly indicate that AtREC8 is required for axis building but is not involved in the stabilisation of axial elements because a normal axis may persist even if AtREC8 dissociates from chromosomes. Furthermore, these results clearly show that the stabilisation of AtREC8 on chromatin needs both proteins AtSCC3 and AtSPO11-1 to be present. However, it is impossible to determine whether this stabilisation involves SPO11-mediated DSBs or another role of SPO11. There must be some kind of redundancy between AtSPO11 and AtSCC3 in stabilisation of the cohesin complex as the destabilisation of AtREC8 was observed only in the *Atspo11-1-Atscc3-1* double mutant. In yeast, Spo11 has been shown to perform functions other than initiating DSB formation in meiotic prophase (normal S-phase length and early homologue pairing) (Cha et al., 2000). Spo11 has also been shown to be associated with the entire length of the chromosome axis in mouse (Romanienko and Camerini-Otero, 2000) and in *Sordaria*, Spo11-GFP staining gives a linear signal along chromosomes during the bouquet stage (Storz et al., 2003), suggesting possible alternative roles of Spo11 in these organisms as well.

In conclusion, we have identified the *Arabidopsis* SCC3 cohesin and demonstrated that it is involved both in meiotic and mitotic divisions. In meiosis, both AtSCC3 and AtREC8 are necessary for kinetochore orientation and centromere cohesion at anaphase I but not for arm and centromere cohesion until metaphase I. It is striking to note that although some organisms possess a single copy of *Scs3* (*S. cerevisiae*, *C. elegans* and *A. thaliana*) others have additional *Scs3* homologues (*S. pombe*, mammals and *D. melanogaster*) and have diversified *Scs3* functions, these differences are without any obvious link with either species proximity, genome size or chromosome number. It remains to be seen if organisms lacking an additional meiotic *Scs3* homolog have selected another unrelated protein to provide some cohesin function in place of meiotic *Scs3* or if the sole *Scs3* protein deals with the specific meiotic *Scs1* homolog (Rec8).

We are grateful to Georges Pelletier, Ivan Le Masson and Fabien Nogué for helpful discussions and critical reading of the manuscript. We thank H. Offenberger and C. Heyting for providing RAD51 antibody, C. Franklin for ASY1 antibody and C. Makaroff for SYN1 antibody. We also wish to thank all the *Arabidopsis* group members for their help in screening the T-DNA transformant collection of Versailles. We thank Halima Morin for technical advice.

References

- Alonso, J. M., Stepanova, A. N., Leisse, T. J., Kim, C. J., Chen, H., Shinn, P., Stevenson, D. K., Zimmerman, J., Barajas, P., Cheuk, R. et al. (2003). Genome-wide insertional mutagenesis of *Arabidopsis thaliana*. *Science* **301**, 653-657.
- Altschul, S. F., Gish, W., Miller, W., Myers, E. W. and Lipman, D. J. (1990). Basic local alignment search tool. *J. Mol. Biol.* **215**, 403-410.
- Anderson, D. E., Losada, A., Erickson, H. P. and Hirano, T. (2002). Condensin and cohesin display different arm conformations with characteristic hinge angles. *J. Cell Biol.* **156**, 419-424.
- Anderson, L. K., Offenberger, H. H., Verkuijlen, W. M. and Heyting, C. (1997). RecA-like proteins are components of early meiotic nodules in lily. *Proc. Natl. Acad. Sci. USA* **94**, 6868-6873.
- Armstrong, S. J., Caryl, A. P., Jones, G. H. and Franklin, F. C. (2002). Asy1, a protein required for meiotic chromosome synapsis, localizes to axis-associated chromatin in *Arabidopsis* and *Brassica*. *J. Cell Sci.* **115**, 3645-3655.
- Bai, X., Peirson, B. N., Dong, F., Xue, C. and Makaroff, C. A. (1999). Isolation and characterization of SYN1, a RAD21-like gene essential for meiosis in *Arabidopsis*. *Plant Cell* **11**, 417-430.
- Bannister, L. A., Reinholdt, L. G., Munroe, R. J. and Schimenti, J. C. (2004). Positional cloning and characterization of mouse *mei8*, a disrupted allele of the meiotic cohesin *Rec8*. *Genesis* **40**, 184-194.
- Bechtold, N., Ellis, J. and Pelletier, G. (1993). In planta *Agrobacterium* mediated gene transfer by infiltration of adult *Arabidopsis thaliana* plants. *C. R. Acad. Sci. Paris* **316**, 1194-1199.
- Bhatt, A. M., Lister, C., Page, T., Franz, P., Findlay, K., Jones, G. H., Dickinson, H. G. and Dean, C. (1999). The DIF1 gene of *Arabidopsis* is required for meiotic chromosome segregation and belongs to the REC8/RAD21 cohesin gene family. *Plant J.* **19**, 463-472.
- Cai, X., Dong, F., Edelmann, R. E. and Makaroff, C. A. (2003). The *Arabidopsis* SYN1 cohesin protein is required for sister chromatid arm cohesion and homologous chromosome pairing. *J. Cell Sci.* **116**, 2999-3007.
- Cha, R. S., Weiner, B. M., Keeney, S., Dekker, J. and Kleckner, N. (2000). Progression of meiotic DNA replication is modulated by interchromosomal interaction proteins, negatively by Spo11p and positively by Rec8p. *Genes Dev.* **14**, 493-503.
- DeVeaux, L. C. and Smith, G. R. (1994). Region-specific activators of meiotic recombination in *Schizosaccharomyces pombe*. *Genes Dev.* **8**, 203-210.
- Dong, F., Cai, X. and Makaroff, C. A. (2001). Cloning and characterization of two *Arabidopsis* genes that belong to the RAD21/REC8 family of chromosome cohesin proteins. *Gene* **271**, 99-108.
- Eijpe, M., Heyting, C., Gross, B. and Jessberger, R. (2000). Association of mammalian SMC1 and SMC3 proteins with meiotic chromosomes and synaptonemal complexes. *J. Cell Sci.* **113**, 673-682.
- Eijpe, M., Offenberger, H., Jessberger, R., Revenkova, E. and Heyting, C. (2003). Meiotic cohesin REC8 marks the axial elements of rat synaptonemal complexes before cohesins SMC1beta and SMC3. *J. Cell Biol.* **160**, 657-670.
- Estelle, M. A. and Somerville, C. (1987). Auxin-resistant mutants of *Arabidopsis thaliana* with an altered morphology. *Mol. Gen. Genet.* **206**, 200-206.
- Franklin, A. E., McElver, J., Sunjevaric, I., Rothstein, R., Bowen, B. and Cande, W. Z. (1999). Three-dimensional microscopy of the Rad51 recombination protein during meiotic prophase. *Plant Cell* **11**, 809-824.
- Grelon, M., Vezon, D., Gendrot, G. and Pelletier, G. (2001). AtSPO11-1 is necessary for efficient meiotic recombination in plants. *EMBO J.* **20**, 589-600.
- Gruber, S., Haering, C. H. and Nasmyth, K. (2003). Chromosomal cohesin forms a ring. *Cell* **112**, 765-777.
- Haering, C. H. and Nasmyth, K. (2003). Building and breaking bridges between sister chromatids. *BioEssays* **25**, 1178-1191.
- Haering, C. H., Lowe, J., Hochwagen, A. and Nasmyth, K. (2002). Molecular architecture of SMC proteins and the yeast cohesin complex. *Mol. Cell* **9**, 773-788.
- Hartung, F., Angelis, K. J., Meister, A., Schubert, I., Melzer, M. and Puchta, H. (2002). An archaeobacterial topoisomerase homolog not present in other eukaryotes is indispensable for cell proliferation of plants. *Curr. Biol.* **12**, 1787-1791.
- Katis, V. L., Galova, M., Rabitsch, K. P., Gregan, J. and Nasmyth, K. (2004). Maintenance of cohesin at centromeres after meiosis I in budding yeast requires a kinetochore-associated protein related to MEI-S332. *Curr. Biol.* **14**, 560-572.
- Keeney, S. (2001). Mechanism and control of meiotic recombination initiation. *Curr. Top. Dev. Biol.* **52**, 1-53.
- Kitajima, T. S., Yokobayashi, S., Yamamoto, M. and Watanabe, Y. (2003). Distinct cohesin complexes organize meiotic chromosome domains. *Science* **300**, 1152-1155.
- Kitajima, T. S., Kawashima, S. A. and Watanabe, Y. (2004). The conserved kinetochore protein shugoshin protects centromeric cohesion during meiosis. *Nature* **427**, 510-517.

- Klein, F., Mahr, P., Galova, M., Buonomo, S. B., Michaelis, C., Nairz, K. and Nasmyth, K. (1999). A central role for cohesins in sister chromatid cohesion, formation of axial elements, and recombination during yeast meiosis. *Cell* **98**, 91-103.
- Krawchuk, M. D. and Wahls, W. P. (1999). Centromere mapping functions for aneuploid meiotic products: Analysis of *rec8*, *rec10* and *rec11* mutants of the fission yeast *Schizosaccharomyces pombe*. *Genetics* **153**, 49-55.
- Leong, A. S. and Sormunen, R. T. (1998). Microwave procedures for electron microscopy and resin-embedded sections. *Micron* **29**, 397-409.
- Losada, A., Hirano, M. and Hirano, T. (1998). Identification of *Xenopus* SMC protein complexes required for sister chromatid cohesion. *Genes Dev.* **12**, 1986-1997.
- Losada, A., Yokochi, T., Kobayashi, R. and Hirano, T. (2000). Identification and characterization of SA/ScC3p subunits in the *Xenopus* and human cohesin complexes. *J. Cell Biol.* **150**, 405-416.
- Marston, A. L., Tham, W. H., Shah, H. and Amon, A. (2004). A genome-wide screen identifies genes required for centromeric cohesion. *Science* **303**, 1367-1370.
- Masson, J. Y. and West, S. C. (2001). The Rad51 and Dmc1 recombinases: a non-identical twin relationship. *Trends Biochem. Sci.* **26**, 131-136.
- Mercier, R., Vezon, D., Bullier, E., Motamayor, J. C., Sellier, A., Lefevre, F., Pelletier, G. and Horlow, C. (2001). SWITCH1 (SWI1): a novel protein required for the establishment of sister chromatid cohesion and for bivalent formation at meiosis. *Genes Dev.* **15**, 1859-1871.
- Mercier, R., Armstrong, S. J., Horlow, C., Jackson, N. P., Makaroff, C. A., Vezon, D., Pelletier, G., Jones, G. H. and Franklin, F. C. (2003). The meiotic protein SWI1 is required for axial element formation and recombination initiation in *Arabidopsis*. *Development* **130**, 3309-3318.
- Molnar, M., Doll, E., Yamamoto, A., Hiraoka, Y. and Kohli, J. (2003). Linear element formation and their role in meiotic sister chromatid cohesion and chromosome pairing. *J. Cell Sci.* **116**, 1719-1731.
- Nasmyth, K. (2002). Segregating sister genomes: the molecular biology of chromosome separation. *Science* **297**, 559-565.
- Parra, M. T., Viera, A., Gomez, R., Page, J., Benavente, R., Santos, J. L., Rufas, J. S. and Suja, J. A. (2004). Involvement of the cohesin Rad21 and SCP3 in monopolar attachment of sister kinetochores during mouse meiosis I. *J. Cell Sci.* **117**, 1221-1234.
- Pasierbek, P., Jantsch, M., Melcher, M., Schleiffer, A., Schweizer, D. and Loidl, J. (2001). A *Caenorhabditis elegans* cohesion protein with functions in meiotic chromosome pairing and disjunction. *Genes Dev.* **15**, 1349-1360.
- Pasierbek, P., Fodermayr, M., Jantsch, V., Jantsch, M., Schweizer, D. and Loidl, J. (2003). The *Caenorhabditis elegans* SCC-3 homologue is required for meiotic synapsis and for proper chromosome disjunction in mitosis and meiosis. *Exp. Cell Res.* **289**, 245-255.
- Pezzi, N., Prieto, I., Kremer, L., Perez Jurado, L. A., Valero, C., Del Mazo, J., Martinez, A. C. and Barbero, J. L. (2000). STAG3, a novel gene encoding a protein involved in meiotic chromosome pairing and location of STAG3-related genes flanking the Williams-Beuren syndrome deletion. *FASEB J.* **14**, 581-592.
- Prieto, I., Suja, J. A., Pezzi, N., Kremer, L., Martinez, A. C., Rufas, J. S. and Barbero, J. L. (2001). Mammalian STAG3 is a cohesin specific to sister chromatid arms in meiosis I. *Nat. Cell Biol.* **3**, 761-766.
- Rabitsch, K. P., Petronczki, M., Javerzat, J. P., Genier, S., Chwalla, B., Schleiffer, A., Tanaka, T. U. and Nasmyth, K. (2003). Kinetochores recruitment of two nucleolar proteins is required for homolog segregation in meiosis I. *Dev. Cell* **4**, 535-548.
- Revenkova, E., Eijpe, M., Heyting, C., Hodges, C. A., Hunt, P. A., Liebe, B., Scherthan, H. and Jessberger, R. (2004). Cohesin SMC1 beta is required for meiotic chromosome dynamics, sister chromatid cohesion and DNA recombination. *Nat. Cell Biol.* **6**, 555-562.
- Romanienko, P. J. and Camerini-Otero, R. D. (2000). The mouse Spo11 gene is required for meiotic chromosome synapsis. *Mol. Cell* **6**, 975-987.
- Ross, K. J., Fransz, P. and Jones, G. H. (1996). A light microscopic atlas of meiosis in *Arabidopsis thaliana*. *Chromosome Res.* **4**, 507-516.
- Storlazzi, A., Tesse, S., Gargano, S., James, F., Kleckner, N. and Zickler, D. (2003). Meiotic double-strand breaks at the interface of chromosome movement, chromosome remodeling, and reductional division. *Genes Dev.* **17**, 2675-2687.
- Tatusova, T. A. and Madden, T. L. (1999). BLAST 2 Sequences, a new tool for comparing protein and nucleotide sequences. *FEMS Microbiol. Lett.* **174**, 247-250.
- Terasawa, M., Shinohara, A., Hotta, Y., Ogawa, H. and Ogawa, T. (1995). Localization of RecA-like recombination proteins on chromosomes of the lily at various meiotic stages. *Genes Dev.* **9**, 925-934.
- Tomonaga, T., Nagao, K., Kawasaki, Y., Furuya, K., Murakami, A., Morishita, J., Yuasa, T., Sutani, T., Kearsy, S. E., Uhlmann, F. et al. (2000). Characterization of fission yeast cohesin: essential anaphase proteolysis of Rad21 phosphorylated in the S phase. *Genes Dev.* **14**, 2757-2770.
- Toth, A., Ciosk, R., Uhlmann, F., Galova, M., Schleiffer, A. and Nasmyth, K. (1999). Yeast cohesin complex requires a conserved protein, Eco1p(Ctf7), to establish cohesion between sister chromatids during DNA replication. *Genes Dev.* **13**, 320-333.
- Toth, A., Rabitsch, K. P., Galova, M., Schleiffer, A., Buonomo, S. B. and Nasmyth, K. (2000). Functional genomics identifies monopolin: a kinetochore protein required for segregation of homologs during meiosis I. *Cell* **103**, 1155-1168.
- van Heemst, D. and Heyting, C. (2000). Sister chromatid cohesion and recombination in meiosis. *Chromosoma* **109**, 10-26.
- Vass, S., Cotterill, S., Valdeolmillos, A. M., Barbero, J. L., Lin, E., Warren, W. D. and Heck, M. M. (2003). Depletion of Drad21/ScC1 in *Drosophila* cells leads to instability of the cohesin complex and disruption of mitotic progression. *Curr. Biol.* **13**, 208-218.
- Waizenegger, I. C., Hauf, S., Meinke, A. and Peters, J. M. (2000). Two distinct pathways remove mammalian cohesin from chromosome arms in prophase and from centromeres in anaphase. *Cell* **103**, 399-410.
- Wang, F., Yoder, J., Antoshechkin, I. and Han, M. (2003). *Caenorhabditis elegans* EVL-14/PDS-5 and SCC-3 are essential for sister chromatid cohesion in meiosis and mitosis. *Mol. Cell Biol.* **23**, 7698-7707.
- Watanabe, Y. (2004). Modifying sister chromatid cohesion for meiosis. *J. Cell Sci.* **117**, 4017-4023.
- Watanabe, Y. and Nurse, P. (1999). Cohesin Rec8 is required for reductional chromosome segregation at meiosis. *Nature* **400**, 461-464.
- Watanabe, Y., Yokobayashi, S., Yamamoto, M. and Nurse, P. (2001). Pre-meiotic S phase is linked to reductional chromosome segregation and recombination. *Nature* **409**, 359-363.
- Xu, H., Beasley, M. D., Warren, W. D., van der Horst, G. T. J. and McKay, M. J. (2005). Absence of mouse REC8 cohesin promotes synapsis of sister chromatids in meiosis. *Dev. Cell* **8**, 949-961.
- Yokobayashi, S., Yamamoto, M. and Watanabe, Y. (2003). Cohesins determine the attachment manner of kinetochores to spindle microtubules at meiosis I in fission yeast. *Mol. Cell Biol.* **23**, 3965-3973.